haematologica
Journal of the Ferrata Storti Foundation

Repurposing CD19-directed immunotherapies for pediatric t(8;21) acute myeloid leukemia

by Farnaz Barneh, Joost B. Koedijk, Noa E. Wijnen, Tom Meulendijks, Minoo Ashtiani, Ester Dunnebach, Noël Dautzenberg, Annelisa M. Cornel, Anja Krippner-Heidenreich, Kim Klein, C. Michel Zwaan, Jürgen Kuball, Stefan Nierkens, Jacqueline Cloos, Gertjan J.L. Kaspers, and Olaf Heidenreich

Received: April 18, 2024.
Accepted: July 30, 2024.

Citation: Farnaz Barneh, Joost B. Koedijk, Noa E. Wijnen, Tom Meulendijks, Minoo Ashtiani, Ester Dunnebach, Noël Dautzenberg, Annelisa M. Cornel, Anja Krippner-Heidenreich, Kim Klein, C. Michel Zwaan, Jürgen Kuball, Stefan Nierkens, Jacqueline Cloos, Gertjan J.L. Kaspers, and Olaf Heidenreich. Repurposing CD19-directed immunotherapies for pediatric t(8;21) acute myeloid leukemia.
Haematologica. 2024 Aug 8. doi: 10.3324/haematol.2024.285707 [Epub ahead of print]

Letter to the editor

Repurposing CD19-directed immunotherapies for pediatric t(8;21) acute myeloid leukemia

Farnaz Barneh[1#], Joost B. Koedijk[1,2#], Noa E. Wijnen[1,3#], Tom Meulendijks[1], Minoo Ashtiani[1], Ester Dunnebach[1,4], Noël Dautzenberg[1], Annelisa M. Cornel[1,4], Anja Krippner-Heidenreich[1], Kim Klein[1,5], C. Michel Zwaan[1,2], Jürgen Kuball[4], Stefan Nierkens[1,4], Jacqueline Cloos[6], Gertjan J.L. Kaspers[1,3]*, Olaf Heidenreich[1,7,8]*

[#]Shared first-authorship; *Shared senior-authorship

1. Princess Máxima Center for Pediatric Oncology, Utrecht, The Netherlands
2. Erasmus MC-Sophia Children's Hospital, Department of Pediatric Oncology, Rotterdam, The Netherlands
3. Emma Children's Hospital, Amsterdam UMC, Vrije Universiteit, Department of Pediatric Oncology, Amsterdam, The Netherlands
4. Center for Translational Immunology, University Medical Center Utrecht, Utrecht University, Utrecht, The Netherlands
5. Wilhelmina Children's Hospital/University Medical Center, Utrecht, The Netherlands
6. Department of Hematology, Amsterdam UMC, Location VUMC, Cancer Center Amsterdam, The Netherlands
7. Wolfson Childhood Cancer Research Centre, Translational and Clinical Research Institute, Newcastle University, Newcastle upon Tyne, United Kingdom
8. University Medical Center Utrecht, Utrecht University, Utrecht, The Netherlands

Corresponding authors:

G.J.L. Kaspers, Princess Máxima Center for Pediatric Oncology, Heidelberglaan 25, 3584 CS Utrecht, The Netherlands. E-mail: g.j.l.kaspers@prinsesmaximacentrum.nl; Tel: +31889727272

O. Heidenreich, Princess Máxima Center for Pediatric Oncology, Heidelberglaan 25, 3584 CS Utrecht, The Netherlands.E-mail: O.T.Heidenreich@prinsesmaximacentrum.nl; Tel: +31683069960

Short title: Targeting CD19 in pediatric t(8;21) AML

Word count: 1498 **Figures:** 3 main figures, 2 supplementary figures **References:** 15

Disclosures

This work has been funded by a KIKA (329) program grant to O.H.

Zwaan: Kura: Other: Institutional support for clinical trials; Gilead: Other: Institutional support for clinical trials; Novartis: Membership on an entity's Board of Directors or advisory committees; Syndax: Consultancy; Incyte: Consultancy; BMS: Consultancy; Kura Oncology: Consultancy; Jazz: Other: Institutional support for clinical trials; Gilead: Consultancy; Novartis: Consultancy; Daiichi Sankyo: Other: Institutional support for clinical trials; ITCC Hem Malignancies Committee: Other: Leadership or fiduciary role in other board, society, committee, or advocacy group, paid or unpaid; Chair Dutch MREC Society: Other: Leadership or fiduciary role in other board, society, committee, or advocacy group, paid or unpaid; Chair MREC Utrecht: Other: Leadership or fiduciary role in other board, society, committee, or advocacy group, paid or unpaid; Sanofi: Membership on an entity's Board of Directors or advisory committees; Incyte: Membership on an entity's Board of Directors or advisory committees; Takeda: Other: Institutional support for clinical trials; Abbvie: Other: Institutional support for clinical trials; Pfizer: Other: Institutional support for clinical trials.

Heidenreich: Roche: Research Funding; Syndax: Research Funding.

Contributions

F.B., N.W., G.K., and O.H. formulated the study concept and designed experiments. The experiments were performed by F.B., J.B.K., N.W., T.M., M.A., and E.D. CD19-directed CAR T cell generation was performed by N.D., and A.M.C, and was supervised by S.N. and J.K. The AML medium was optimized by A.K.H. Data interpretation was performed by F.B., N.W., and J.B.K. Co-supervising the panel design for identification of leukemic cells in killing assays of primary AML samples was done by J.C. The manuscript was written by F.B, J.B.K., N.W., and

O.H. together with T.M. The study was supervised by K.K., C.Z., G.K., and O.H. All authors read and approved the final version of the manuscript.

Acknowledgements

We thank the patients, parents, and caregivers for their participation. Appreciation goes to Anja de Jong (Prinses Máxima Center) for flow cytometry data, Zinia Kwidama for providing AML samples, Tom Reuvekamp and Marisa Westers for fruitful data discussions (Amsterdam UMC location VUmc, The Netherlands). Zsolt Sebestyen (UMC Utrecht, The Netherlands) provided T-cell expansion feeders for generation of CAR T cells. Figures were created with BioRender.com.

Data-sharing statement

Bulk RNA-sequencing data (count data) generated for this manuscript can be retrieved from the Gene Expression Omnibus (GSE270185). Requests for raw sequencing data should be addressed to the corresponding authors.

The development of targeted immunotherapy for acute myeloid leukemia (AML) has been challenging due to the paucity of tumor-specific antigens, on-target off-leukemia hematological toxicity, and an immunosuppressive tumor microenvironment.[1-4] Repurposing immunotherapies that have been used to target other hematological malignancies could, in case of a shared target antigen, represent a promising opportunity to expand the immunotherapeutic options for AML. CD19, a B-cell marker highly expressed in B-cell precursor acute lymphoblastic leukemia (BCP-ALL), is one such shared target antigen. Indeed, CD19-expression is also characteristic of t(8;21)(q22;q22) AML, the most common translocation in children with this disease. The success of CD19-directed immunotherapies in BCP-ALL[5-7], as well as in two adults with relapsed $CD19^+$ t(8;21) AML[8, 9], prompted us to investigate CD19 as an immunotherapy target in pediatric AML. This study had been approved by the Biobank Data Access Committee of the Princes Máxima Center.

Using diagnostic flow cytometry records of 167 newly diagnosed *de novo* pediatric AML patients, we identified 18 patients with $CD19^+$ AML (11%; 78% male; median age: 10.5 years (range: 1-17); **Figure 1A**). Among these patients, ten had weak CD19-expression (difference (Δ) in CD19 mean fluorescent intensity (MFI) between leukemic and T-cells (as healthy $CD19^-$ controls) of 0.5 to 1 log). In eight patients, the ΔMFI was greater than 1 log-fold. Regarding cytogenetic alterations, 61% (n=11) of $CD19^+$ patients carried the translocation (8;21)(q22;q22); **Figure 1B**). Other cytogenetic alterations included t(9;11)(p22;q23) (n=2), t(16;21)(q24;q22) (n=2), t(1;11)(q21;q23) (n=1), inv(16)(p13;q22) (n=1), and unknown (n=1; **Figure 1B**). In the entire cohort, 21 out of 167 patients had the (8;21) translocation, indicating that 52% of patients with this translocation had $CD19^+$ AML (**Figure 1C**). All 18 patients with $CD19^+$ AML achieved a complete remission by the second induction course, of which five (28%) relapsed (**Figure 1A**). Of these relapsed patients, two retained CD19-positivity and are alive, while three lost CD19-

expression, of which one deceased. This was the only death among patients with $CD19^+$ AML at diagnosis. Intriguingly, three patients with $CD19^-$ AML at diagnosis gained CD19-positivity at relapse (out of 33 relapses in the $CD19^-$ AML group; **Figure 1A**). Their cytogenetic alterations were del(9q) (n=1), del(7q), del(12p), +1q (n=1), and unknown (n=1), with one fatal outcome. These data demonstrate enrichment of CD19-expression in pediatric t(8;21) AML at diagnosis, which can also emerge at relapse in cases that initially had $CD19^-$ AML.

To further characterize the extent of CD19-expression in pediatric t(8;21) AML, we re-analyzed diagnostic bone marrow mononuclear cell (BMMC) flow cytometry data available for six $CD19^+$ patients (#01-06) and one $CD19^-$ (#07) patient with t(8;21) AML. We examined CD19-expression levels on $CD45^{dim}SSC\text{-}A^{low}CD3^-CD20^-CD34^+$ myeloid blasts, using $CD19^-$ bone marrow (BM) T-cells (from patient#01) as healthy negative controls (**Figure 1D**). In two patients (patients#01-02), the CD19 expression showed a unimodal pattern which approximated that of B-cells. This is indicative of high CD19 expression in the majority of leukemic cells. In contrast, the other four patients (patients#03-06) exhibited lower CD19 expression levels with a non-unimodal pattern (**Figure 1D**). We then compared CD19-expression levels in $CD19^+$ t(8;21) AML samples (RL048 patient-derived xenograft (PDX)[10] and BMMCs from patient#08) with two primary BCP-ALL BMMC samples. While the CD19 MFI in AML patient#08 was lower compared to both BCP-ALL samples, the MFI of the AML PDX sample was equal to (patient#02) or even higher (patient#01) than that of the BCP-ALL samples (**Figure 1E**). Next, we analyzed the CD19-expression on different AML subpopulations in AML samples (patient#01, patient#08, and RL048 PDX). Importantly, nearly all $CD34^+CD38^-$ immature progenitors expressed CD19 (**Figure S1A-C**). Furthermore, in patient#01, we identified CD19 to be expressed on putative leukemic stem cells (LSCs; $CD34^+CD38^-CD45RA^+$) but not on normal stem cells ($CD34^+CD38^-CD45RA^-$; **Figure S1A**). Additionally, virtually all $CD34^+CD38^+$ cells, including

$CD34^+CD38^+CD11b^+$ and $CD34^+CD38^+CD11b^-$ cells, were positive for CD19 (**Figure S1A-C**). In summary, although the CD19-expression level among $CD19^+$ AML patients was heterogeneous, in those with unimodal and high CD19-expression, CD19 was expressed on both more and less mature AML cells. These findings encouraged exploration of the *ex vivo* killing efficiency of immunotherapies targeting CD19, including blinatumomab (CD19-directed bispecific T cell-engager) and CD19-directed chimeric antigen receptor (CAR) T cells.

We next wondered whether blinatumomab-mediated AML-T-cell contact could induce T-cell activation. Using genetically engineered Jurkat cells (**Figure 2A**), we observed a dose-dependent increase in the luminescent signal in a co-culture of $CD19^+$ AML PDX (RL048) and Jurkat cells, indicating blinatumomab-mediated CD3-signaling in T-cells (**Figure 2B**). This finding was further validated using an *ex vivo* co-culture of healthy donor T-cells with $CD19^+$ AML PDX cells. The addition of blinatumomab led to significant upregulation of the T-cell activation markers CD25 (50% marker positivity) and CD137 (90% marker positivity; **Figure 2C**). Next, to determine whether AML cells were sensitive to blinatumomab-mediated T-cell cytotoxicity, we treated *ex vivo* co-cultures with 1 nM blinatumomab, which resulted in 40% AML PDX cell killing at a low effector-to-target (E:T)-ratio of 1:10 and almost 90% killing at an E:T-ratio of 1:1 (**Figure 2D**). Notably, absence of allogeneic T-cells or blinatumomab led to no or negligible background killing. We subsequently compared the blinatumomab-mediated T-cell killing efficiency between AML and BCP-ALL samples in *ex vivo* co-cultures with healthy donor T-cells. Intriguingly, although we observed substantial variation in the killing efficiency among the three BCP-ALL samples, the observed AML cell killing was comparable to that of BCP-ALL cells at each E:T ratio ($P>0.05$; **Figure 2E**). We also assessed whether $CD19^+$ t(8;21) AML cells were sensitive to CAR T-cell-mediated cytotoxicity. Similar to blinatumomab, co-culturing CD19-directed CAR T-cells containing a 4-1BB transactivation domain with primary AML cells at a low

E:T-ratio of 1:10 led to 40% killing of AML cells within 48 hours, while AML cells were nearly completely eradicated at an E:T-ratio of 1:1 (**Figure 2F**). AML cell viability remained constant in co-cultures with untransduced T-cells from the same donor, again indicating negligible background killing (**Figure 2F**). Taken together, these findings demonstrate that CD19-directed immunotherapies induce efficient killing of $CD19^+$ AML cells *ex vivo*.

To improve our understanding of the extent of immunosuppression in the BM of pediatric $CD19^+$ t(8;21) AML, we characterized the tumor immune microenvironment using immunogenomic computational approaches applied to diagnostic BM bulk RNA-seq data. Accordingly, we deconvoluted the immune cell abundance in the BM of treatment-naïve $CD19^+$ t(8;21) AML (n=5), $CD19^-$ t(8;21) AML (n=5), other AML genotypes (n=30), and non-leukemic controls (n=4)[11] using CIBERSORTx[12] and the TIDE algorithm[13]. As we did not detect differences between $CD19^+$ and $CD19^-$ t(8;21) AML (**Figure S2A-J**), we considered these cases in aggregate for subsequent comparisons (t(8;21)-group). Similarly, we found no differences in the abundance of microenvironmental subsets between both AML groups and non-leukemic controls, which was also the case for two RNA-based metrics related to immune (dys)function[14, 15] (**Figure S2K-R**). Comparing the BM of pediatric t(8;21) AML (n=10) to that of pediatric BCP-ALL (n=209), we found that BCP-ALL cases had a significantly higher abundance of myeloid-derived suppressor cells (MDSCs; **Figure S2O**). Furthermore, BCP-ALL cases were enriched for T- and NK-cell exhaustion and senescence (**Figure S2L-N**), potentially reflecting a prior T- and NK-cell response rendered dysfunctional. On the other hand, cancer-associated fibroblasts (CAFs), memory B-cells, and plasma cells were significantly increased in t(8;21) AML compared to BCP-ALL (**Figure S2P-R**). Altogether, our immunogenomic approach revealed that the BM microenvironment in pediatric t(8;21) AML is similar to non-leukemic controls but, at least in part, distinct from pediatric BCP-ALL.

Following the deconvolution of the abundance and function of T-cells in the pediatric t(8;21) AML BM, we evaluated the functionality of autologous T-cells in AML and BCP-ALL BMMC samples. Addition of blinatumomab to AML BMMCs (from patients #01 and #08, containing 4% and 8% T-cells, respectively) led, in 48 hours, to a 50% reduction in cell viability (**Figure 3A**). This was comparable to that observed in BCP-ALL samples (all contained 3% autologous CD3 T-cells; $P>0.05$; **Figure 3A**). Moreover, we found that addition of blinatumomab to AML BMMC samples induced a significant increase in IFN-γ secretion compared to BMMCs without blinatumomab, with the extent proportional to the abundance of T-cells in the BM (**Figure 3B**). In addition, the T-cell activation markers CD25 and CD137 on BM T-cells increased substantially in response to blinatumomab (**Figure 3C**), together providing support for the activation of T-cells. For patient#01, matched peripheral blood (PB) was also available, which allowed for a co-culture of PB-derived T-cells with autologous BMMCs. The autologous PB T-cells showed substantial activation upon treatment with blinatumomab (**Figure 3D**) and demonstrated effective AML cell killing (**Figure 3E**), which was accompanied by substantial IFN-γ secretion (**Figure 3F**) and an increased T-cell abundance after treatment (**Figure 3G**). Overall, these findings demonstrate that autologous T-cells from AML patients are capable to induce cytotoxicity upon binding to T-cell-engagers, encouraging the exploitation of CD19 as an immunotherapy target in pediatric $CD19^+$ t(8;21) AML.

Taken together, our study highlights the potential of CD19-directed immunotherapies for pediatric $CD19^+$ AML. Given that immunotherapies work best at a favorable E:T-ratio[1], these therapies may be particularly effective in the minimal residual disease (MRD) setting before allogeneic stem cell transplantation. Additionally, they could serve as alternatives to intensive chemotherapy, for instance in case of severe chemotherapy-induced complications, or as life-prolonging treatments when curative options are no longer viable.

References

1. Subklewe M, Bücklein V, Sallman D, Daver N. Novel immunotherapies in the treatment of AML: is there hope? Hematology Am Soc Hematol Educ Program. 2023;2023(1):691-701.
2. Koedijk JB, van der Werf I, Calkoen FG, et al. Paving the way for immunotherapy in pediatric acute myeloid leukemia: Current knowledge and the way forward. Cancers (Basel). 2021;13(17):4364.
3. Wijnen NE, Koedijk JB, Klein K, et al. Treating CD33-Positive de novo Acute Myeloid Leukemia in Pediatric Patients: Focus on the Clinical Value of Gemtuzumab Ozogamicin. Onco Targets Ther. 2023;16:297-308.
4. Vadakekolathu J, Rutella S. Escape from T-cell-targeting immunotherapies in acute myeloid leukemia. Blood. 2024;143(26):2689-2700.
5. von Stackelberg A, Locatelli F, Zugmaier G, et al. Phase I/phase II study of blinatumomab in pediatric patients with relapsed/refractory acute lymphoblastic leukemia. J Clin Oncol. 2016;34(36):4381-4389.
6. Maude SL, Laetsch TW, Buechner J, et al. Tisagenlecleucel in children and young adults with B-cell lymphoblastic leukemia. N Engl J Med. 2018;378(5):439-448.
7. Kita K, Nakase K, Miwa H, et al. Phenotypical characteristics of acute myelocytic leukemia associated with the t(8;21)(q22;q22) chromosomal abnormality: frequent expression of immature B-cell antigen CD19 together with stem cell antigen CD34. Blood. 1992;80(2):470-477.
8. Plesa A, Labussière-Wallet H, Hayette S, Salles G, Thomas X, Sujobert P. Efficiency of blinatumomab in at (8; 21) acute myeloid leukemia expressing CD19. Haematologica 2019;104(10):e487-e488.
9. Danylesko I, Jacoby E, Yerushalmi R, et al. Remission of acute myeloid leukemia with t (8; 21) following CD19 CAR T-cells. Leukemia. 2020;34(7):1939-1942.
10. Kellaway SG, Potluri S, Keane P, et al. Leukemic stem cells activate lineage inappropriate signalling pathways to promote their growth. Nat Commun. 2024;15(1):1359.
11. Koedijk JB, van Beek TB, Vermeulen MA, et al. Case Report: Immune dysregulation associated with long-lasting regression of a (pre)leukemic clone. Front Immunol. 2023;14:1280885.
12. Newman AM, Steen CB, Liu CL, et al. Determining cell type abundance and expression from bulk tissues with digital cytometry. Nat Biotechnol. 2019;37(7):773-782.
13. Jiang P, Gu S, Pan D, et al. Signatures of T cell dysfunction and exclusion predict cancer immunotherapy response. Nat Med. 2018;24(10):1550-1558.
14. Dufva O, Pölönen P, Brück O, et al. Immunogenomic landscape of hematological malignancies. Cancer Cell. 2020;38(3):380-399.e13.
15. Rutella S, Vadakekolathu J, Mazziotta F, et al. Immune dysfunction signatures predict outcomes and define checkpoint blockade-unresponsive microenvironments in acute myeloid leukemia. J Clin Invest. 2022;132(21):e159579.

Figure legends

Figure 1. CD19-expression among pediatric AML patients. (A) Incidence of CD19-positivity among newly diagnosed and relapsed pediatric AML patients. (B) Cytogenetic alterations observed in $CD19^+$ pediatric AML patients. NA = cytogenetic data not available. (C) Incidence of the t(8;21) subtype across the total cohort, and the incidence of CD19-positivity among all t(8;21) patients. (D) Gating strategy to identify $CD19^+$ populations and their expression levels among $CD45^{dim}SSC\text{-}A^{low}CD34^+$ blasts in the bone marrow (BM) for seven t(8;21) AML patients. CD19-expression on these blasts was compared to the CD19 levels on healthy T-cells (as $CD19^-$ control). The CD19-expression of B-cells is shown as a $CD19^+$ reference. (E) Comparison of CD19-expression between one primary AML sample (patient #08), AML PDX (RL048), and two primary BCP-ALL samples (patient#01-02). ΔMFI in this experiment was calculated by subtracting the MFI of CD19 in stained samples from the CD19 MFI in corresponding unstained samples. MFI: median fluorescence intensity; PDX: patient-derived xenograft.

Figure 2. T-cell activation and AML cell cytotoxicity mediated by blinatumomab and CAR T-cells. (A) Illustration of the engineered Jurkat T-cell activation bioassay. (B) The luminescent signal intensity upon addition of blinatumomab (blin) concentrations to $CD19^+$ AML PDX (P) and Jurkat cells (J; n=2 technical replicates). bead: CD3/CD28 Dynabeads. (C) Induction of activation markers in primary T-cells upon addition of blinatumomab (blin) and/or $CD19^+$ AML PDX cells. (D) Effect of 1nM blinatumomab (marked as B) on the viability of AML PDX cells (T; Target cells) at various effector-to-target (E:T)-ratios using healthy donor T-cells (E; Effector cells) after 48 hours. Data points represent technical replicates. (E) The viability of AML (patient #08 and PDX) and primary BCP-ALL BMMC samples (n=3 different patients) after 48 hours of co-culture with healthy donor T-cells and blinatumomab (marked as B). Data represent mean ±SD. A two-way ANOVA followed by Šídák's multiple comparisons test was performed between each E:T ratio in AML versus BCP-ALL (ns: not significant, $P > 0.05$). (F) The viability of primary AML cells (patient #08) after 48 hours of co-culture with CD19-directed CAR T-cells or untransduced T-cells (UT; as control) at different E:T-ratios. Data points represent technical replicates.

Figure 3. Functionality and cytotoxicity of T-cells from t(8;21) patients. . (A) Cytotoxicity of autologous bone marrow-derived T-cells upon direct addition of 1 nM blinatumomab to bone

marrow mononuclear cells (BMMCs) from AML (n=2) and BCP-ALL (n=3) samples after 48 hours. A t-test was performed to compare the viability of blinatumomab-treated AML versus BCP-ALL samples. (B) Relative (rel.) interferon (IFN)-γ measurement in the supernatant of two BMMC AML samples. Positive control (Pos CTRL): 125 pg/mL of recombinant IFN-γ protein (n= 3 technical replicates for each patient). (C-D) Changes of the activation markers on blinatumomab-treated autologous $CD3^+$ T-cells, either present within BMMC sample (C; patient #08) or derived from peripheral blood (PB) and co-cultured with autologous BMMCs (D; patient #01). (E) Viability of AML BMMC sample (patient#01) following 48 hours of co-culture with autologous PB-derived $CD3^+$ T-cells and 1 nM blinatumomab at various E:T-ratios (n=3 technical replicates). (F) Relative (rel.) IFN-γ measurement in the supernatant of BMMCs from patient #01 upon co-culture with autologous PB-derived T cells at different E:T ratios. The + and ++ for PB and BMMCs in the table beneath indicate E:T ratios of 1:1 and 2:1, respectively. . Absorbance values were normalized to the corresponding value of $CD3^+$ T-cells alone; positive control (Pos CTRL): 125 pg/mL recombinant IFN-γ, n=3 technical replicates. (G) Ratio of $CD3^+$ T-cell numbers after blinatumomab treatment to the corresponding numbers before treatment, in the autologous BMMC and PB-derived T-cell co-cultures (patient#01, 48 hours).

Figure 1

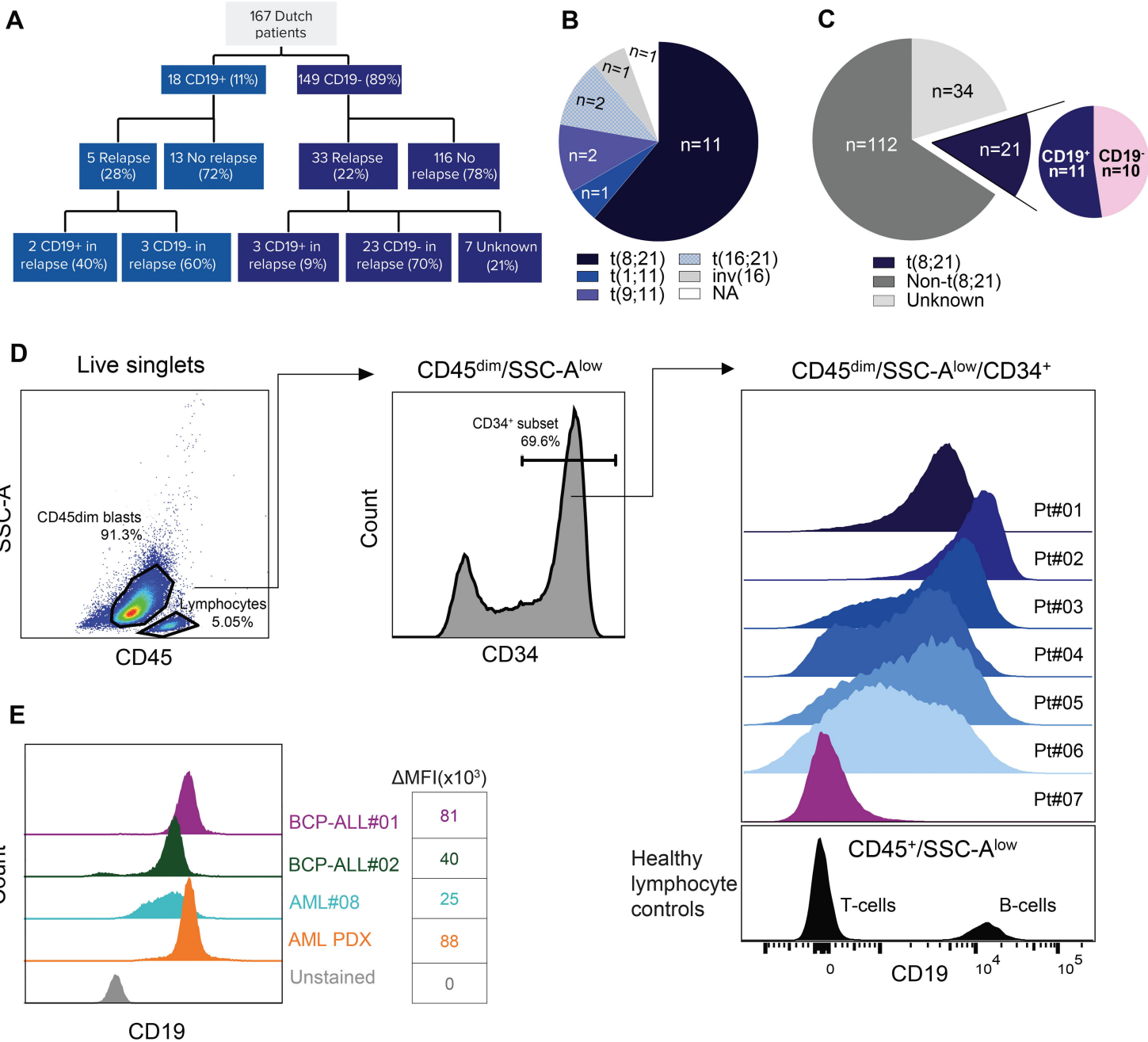
A
167 Dutch patients
18 CD19+ (11%)
149 CD19- (89%)
5 Relapse (28%)
13 No relapse (72%)
33 Relapse (22%)
116 No relapse (78%)
2 CD19+ in relapse (40%)
3 CD19- in relapse (60%)
3 CD19+ in relapse (9%)
23 CD19- in relapse (70%)
7 Unknown (21%)
B
n=11
n=2
n=2
n=1
n=1
t(8;21)
t(1;11)
t(9;11)
t(16;21)
inv(16)
NA
C
n=112
n=34
n=21
CD19+ n=11
CD19- n=10
t(8;21)
Non-t(8;21)
Unknown
D
Live singlets
SSC-A
CD45dim blasts 91.3%
Lymphocytes 5.05%
CD45
CD45dim/SSC-Alow
CD34+ subset 69.6%
Count
CD34
CD45dim/SSC-Alow/CD34+
Pt#01
Pt#02
Pt#03
Pt#04
Pt#05
Pt#06
Pt#07
Healthy lymphocyte controls
CD45+/SSC-Alow
T-cells
B-cells
0
CD19
10^4
10^5
E
Count
BCP-ALL#01
BCP-ALL#02
AML#08
AML PDX
Unstained
ΔMFI(x10^3)
81
40
25
88
0
CD19

Figure 2

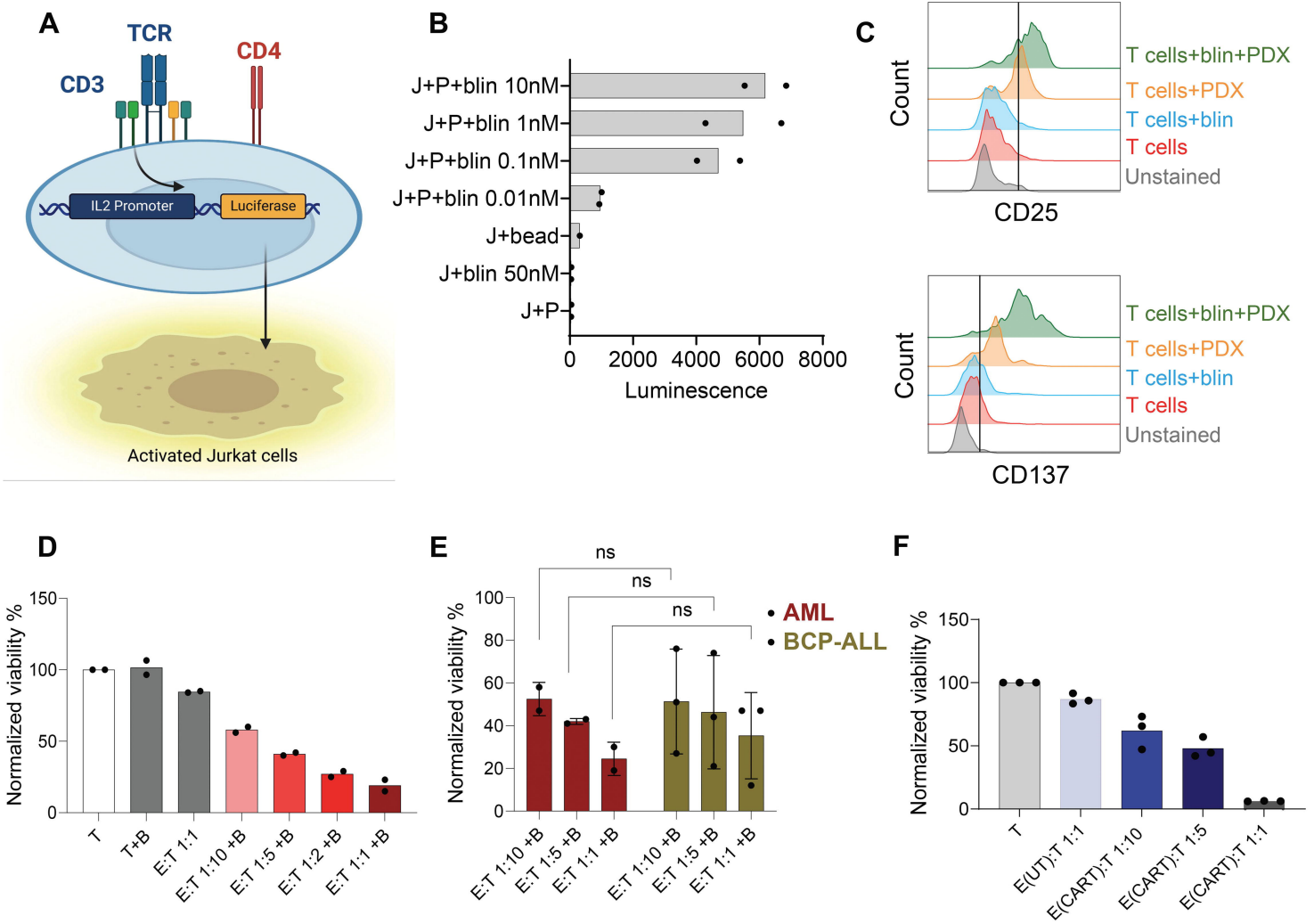
A
TCR
CD4
CD3
IL2 Promoter
Luciferase
Activated Jurkat cells
B
J+P+blin 10nM
J+P+blin 1nM
J+P+blin 0.1nM
J+P+blin 0.01nM
J+bead
J+blin 50nM
J+P
0
2000
4000
6000
8000
Luminescence
C
Count
T cells+blin+PDX
T cells+PDX
T cells+blin
T cells
Unstained
CD25
Count
T cells+blin+PDX
T cells+PDX
T cells+blin
T cells
Unstained
CD137
D
Normalized viability %
150
100
50
0
T
T+B
E:T 1:1
E:T 1:10 +B
E:T 1:5 +B
E:T 1:2 +B
E:T 1:1 +B
E
Normalized viability %
100
80
60
40
20
0
ns
ns
ns
AML
BCP-ALL
E:T 1:10 +B
E:T 1:5 +B
E:T 1:1 +B
E:T 1:10 +B
E:T 1:5 +B
E:T 1:1 +B
F
Normalized viability %
150
100
50
0
T
E(UT):T 1:1
E(CART):T 1:10
E(CART):T 1:5
E(CART):T 1:1

Figure 3

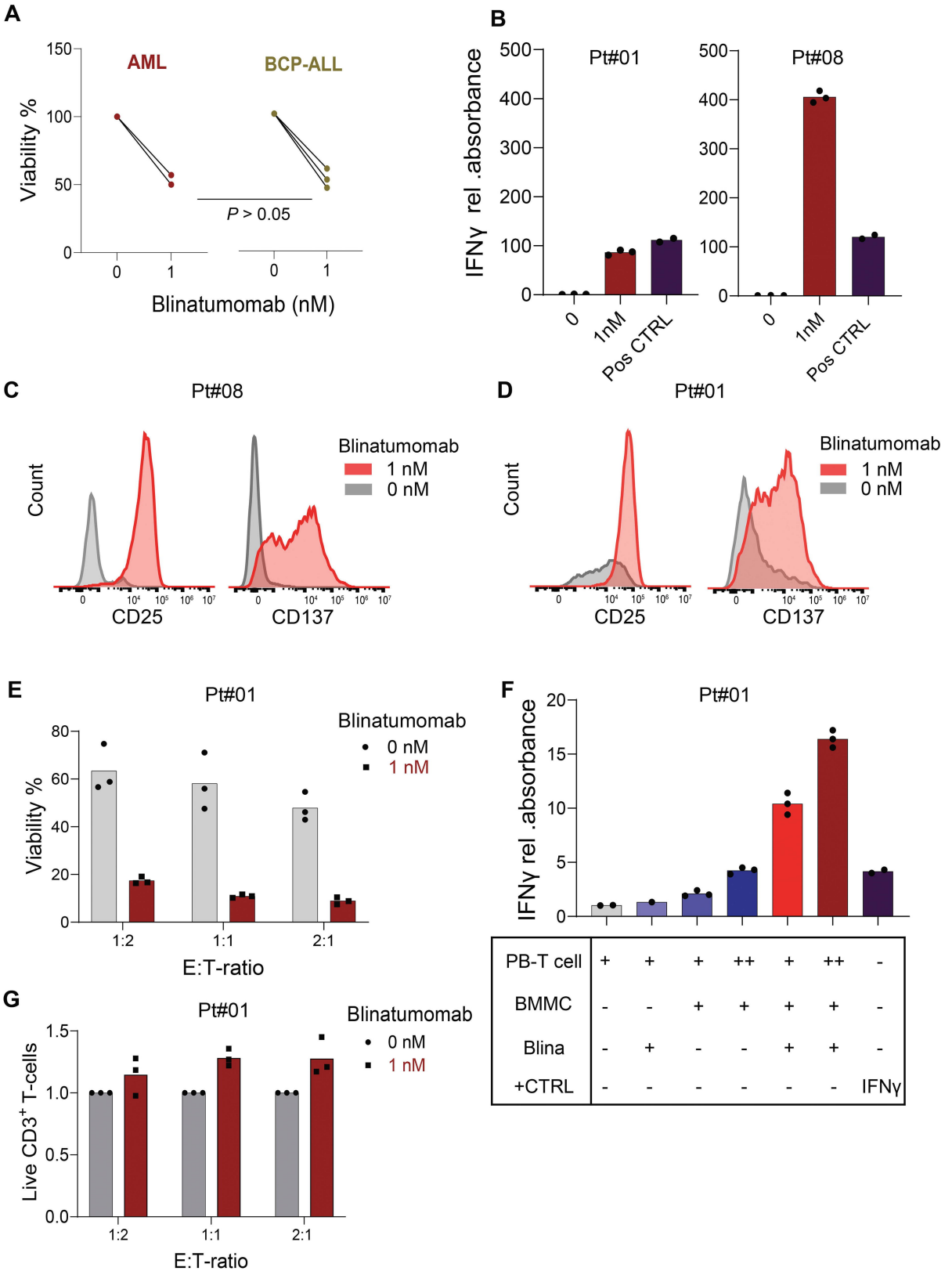
A
AML
BCP-ALL
Viability %
150
100
50
0
P > 0.05
0
1
0
1
Blinatumomab (nM)
B
Pt#01
Pt#08
IFNγ rel .absorbance
500
400
300
200
100
0
0
1nM
Pos CTRL
C
Pt#08
Count
Blinatumomab
1 nM
0 nM
CD25
CD137
D
Pt#01
E
Pt#01
Viability %
80
60
40
20
0
1:2
1:1
2:1
E:T-ratio
F
Pt#01
IFNγ rel .absorbance
20
15
10
5
0
PB-T cell + + + ++ + ++ -
BMMC - - + + + + -
Blina - + - - + + -
+CTRL - - - - - - IFNγ
G
Pt#01
Live CD3+ T-cells
1.5
1.0
0.5
0.0
1:2
1:1
2:1
E:T-ratio

Supplementary Figure 1

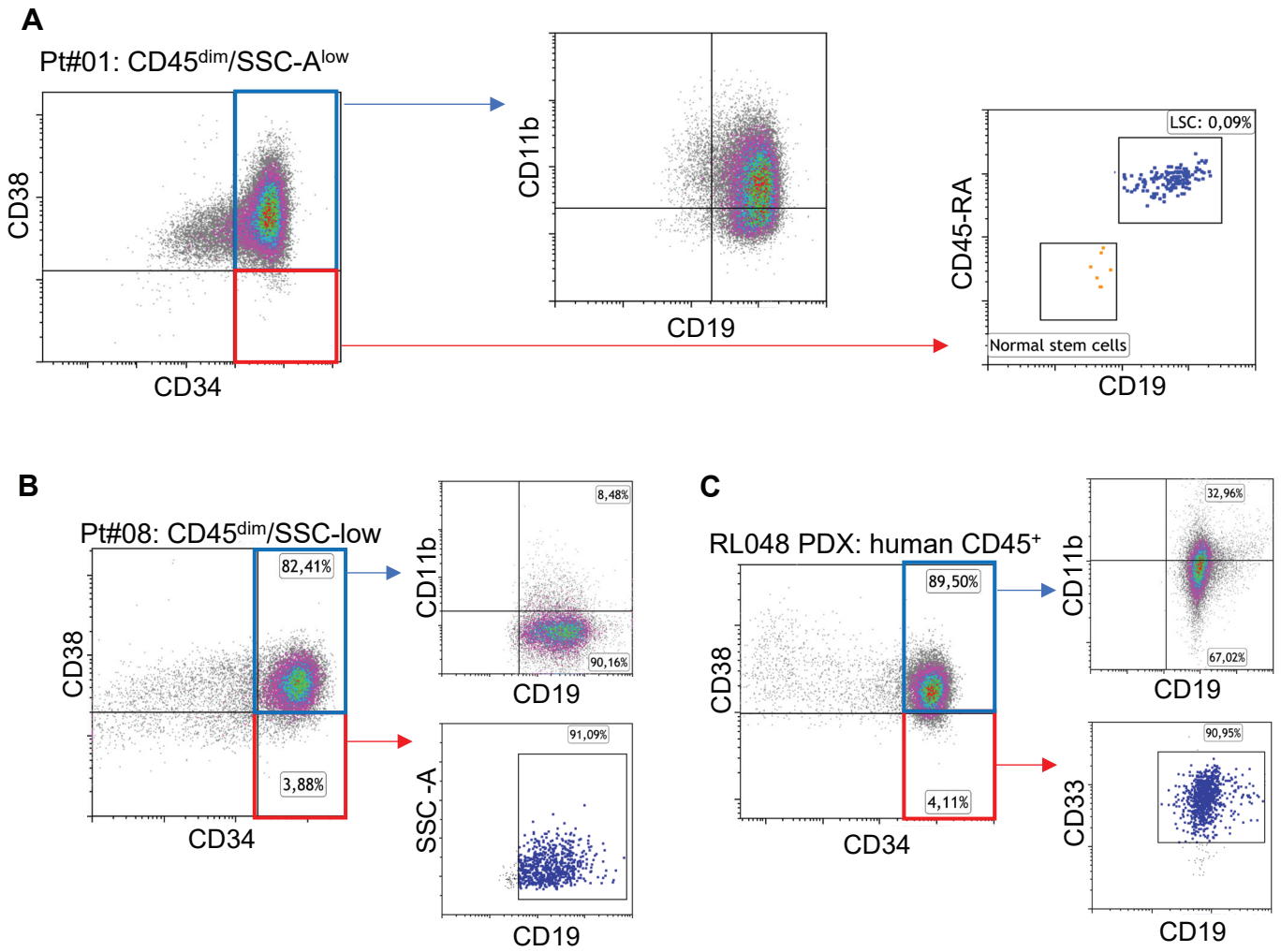

Supplementary Figure 2

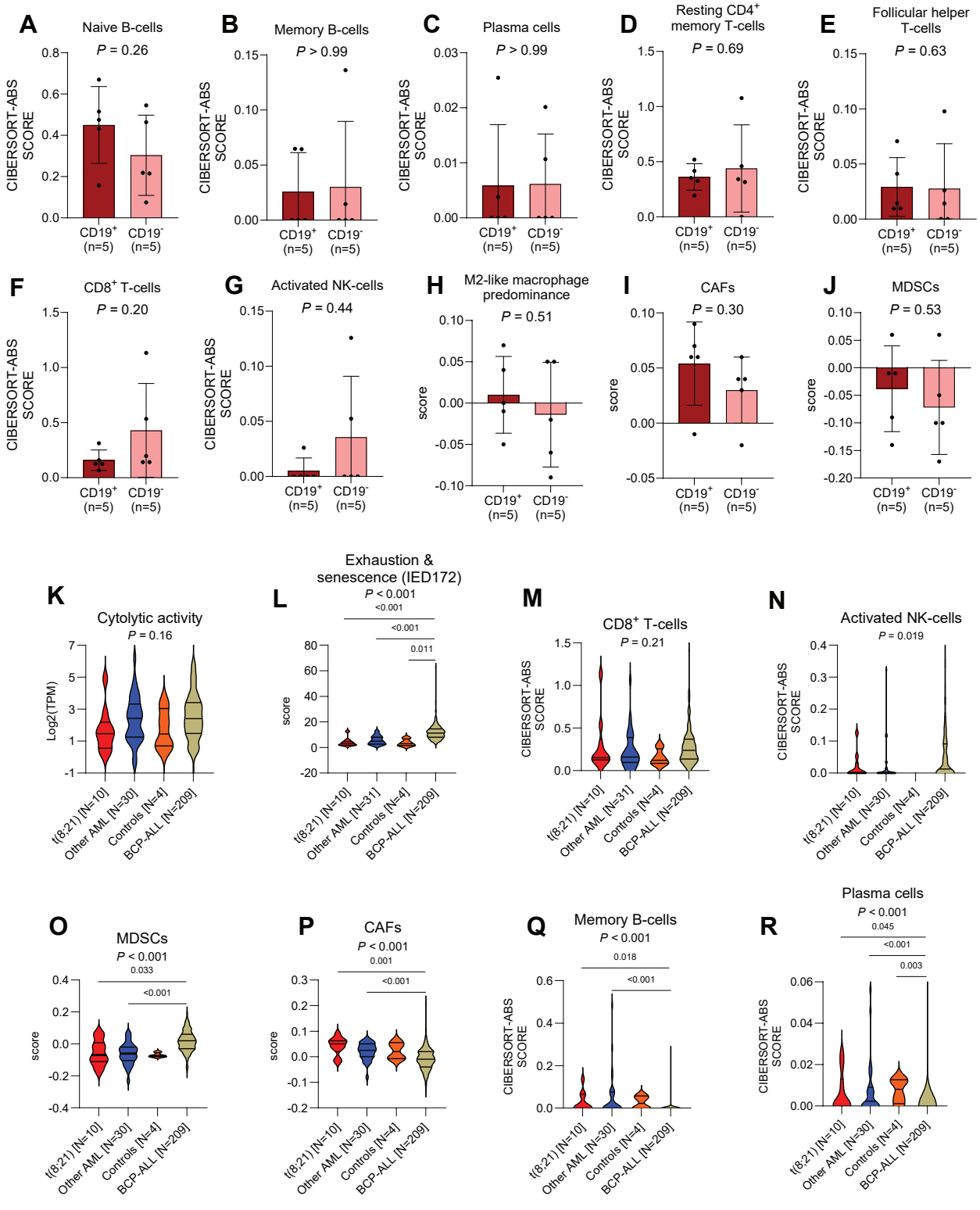

Supplementary Figure legends

Supplementary Figure 1. CD19-expression on AML subpopulations. (A) CD19-expression among putative leukemic stem cells (LSCs; $CD34^+CD38^-CD45RA^+$) and more mature subpopulations ($CD34^+CD38^+CD11b^+$, $CD34^+CD38^+CD11b^-$) from patient #01. (B) CD19-expression among $CD34^+CD38^-$ and more mature subpopulations ($CD34^+CD38^+CD11b^+$, $CD34^+CD38^+CD11b^-$) from patient #08. (C) CD19-expression among $CD34^+CD38^-$ and more mature subpopulations ($CD34^+CD38^+CD11b^+$, $CD34^+CD38^+CD11b^-$) from RL048 PDX cells.

Supplementary Figure 2. Characterization of the bone marrow immune microenvironment of t(8;21) AML using immunogenomic analyses. (A-J) Comparison of the deconvoluted absolute (ABS) abundance of various cell populations among $CD19^+$ and $CD19^-$ t(8;21) AML. Data are presented as mean with standard deviation. The Mann-Whitney test was used to test for statistical differences between groups. (K-R) Comparison of gene signature scores (cytolytic activity[1]: *GZMA, GZMB, PRF1, GNLY, GZMH* (K) and IED172: 172-gene immune effector dysfunction signature[2] (L)) and the absolute abundance of various cell populations among t(8;21) AML patients, AML patients with other cytogenetic alterations, non-leukemic controls, and BCP-ALL patients (all treatment-naïve). Data are presented as median with quartiles and range. Kruskal-Wallis test with Dunn's post-hoc test is performed for multiple comparisons. In case multiple *P* values are shown, the upper one indicates the result of the Kruskal-Wallis test and the lower one(s) the result of Dunn's test. M2-like macrophage predominance: ratio of M2- to M1-like macrophages; NK: natural killer; MDSC: myeloid-derived suppressor cell; CAF: cancer-associated fibroblast.

References

1. Dufva O, Pölönen P, Brück O, et al. Immunogenomic landscape of hematological malignancies. Cancer Cell 2020;38:380-399. e13.

2. Rutella S, Vadakekolathu J, Mazziotta F, et al. Immune dysfunction signatures predict outcomes and define checkpoint blockade–unresponsive microenvironments in acute myeloid leukemia. The Journal of Clinical Investigation 2022;132.

(Reference 14 and 15, respectively, in the main file)